Thermally Slumping Glass for the X-ray Optics of the International Axion Observatory
REU Program at Columbia University - Nevis Labs

Treya Pember[1]

[1]Wellesley College

August 2, 2024

Nevis Laboratories
Columbia University

Abstract

The International Axion Observatory (IAXO) and its prototype, BabyIAXO, promise to set new limits on the search for the axion, a compelling dark matter candidate. IAXO is designed to convert solar axions into X-ray photons using a strong magnetic field. The Perez Lab at Columbia University will contribute to the next-generation experiment by constructing the X-ray optics that will focus these converted photons onto the experiment's detector. The X-ray optics will feature a Wolter 1 telescope design that reflects photons at grazing incidence angles with segmented cylindrical glass substrates. I experimentally derived slumping techniques to form these cylindrical substrates, producing quality glass pieces in 74% of trials.

Contents

1 Background

1.1 Dark Matter and Axions

Based on gravitational interactions, dark matter is five times as prevalent as the luminous matter that makes up the visible universe. Yet, its limited interactions with light mean dark matter is difficult to observe and characterize with conventional methods, making it one of the greatest mysteries facing physics today. The evidence for dark matter is overwhelming, in rotational velocities of galaxies, gravitational lensing observations, and galactic clusters. Dark matter evidence found within the cosmic microwave background demonstrates its significant gravitational influence on the structure of the universe, on a time scale of billions of years, indicating that dark matter must be stable. Any potential dark matter particle must also be massive in order to interact gravitationally.

The axion is a theoretical light-weight weakly interacting particle, a compelling dark matter candidate. Axions originate from an explanation for the strong charge parity (CP) problem within the standard model of particle physics. The strong CP problem questions why a charge parity symmetry violation is seen in the weak force, but not in the strong force. If there were a charge parity symmetry violation in the strong force, it would cause an electric dipole moment within the neutron, an effect which has never been experimentally observed. The Peccei-Quinn Mechanism is a theory which explains this lack of observable symmetry violation, cancelling the theorized electric dipole moment and introducing a new particle, the axion [5].

Axion-like-particles (ALPs) are theoretical particles that occupy a similar mass regime as axions but do not have the mass to coupling strength relationship required to solve the strong CP problem. ALPs are also possible dark matter candidates and are predicted by string theory. Detecting either axions or ALPs would have major implications for our understanding of physics beyond the standard model [1].

Axions and ALPs are theorized to interact with light under special circumstances, converting into a photon, or from a photon, in the presence of a strong magnetic field via a process known as the Primakoff effect (Fig. 1). The Primakoff effect can be exploited by detection experiments that look for excess photons that could be converted axions. One such experimental design is the axion helioscope, which operates under the assumption that stars produce large quantities of axions via the Primakoff effect. X-ray photons in the stellar core convert into axions due to the star's strong electromagnetic fields. These axions stream out of the sun, and when some reach Earth, a helioscope uses a large magnet to reconvert the axions back into X-ray photons and detect them [1].

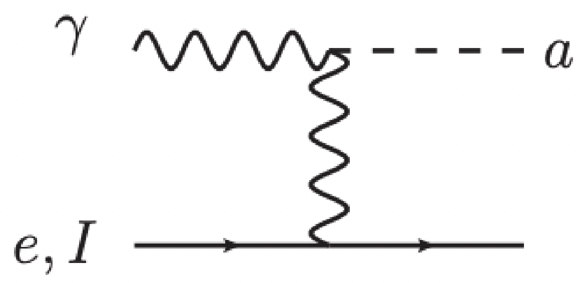

Figure 1: *Feynman Diagram of the Primakoff Effect [1]*

1.2 IAXO Design

The International Axion Observatory (IAXO) is a proposed large-scale helioscope experiment that will track the sun in search of axions and ALPs. BabyIAXO is the prototype experiment for IAXO and will test all of the major systems required for IAXO. BabyIAXO will have the capabilities to improve upon current sensitivity constraints for axions by a factor of five, with IAXO offering an improvement of a factor of twenty. Both experiments will be capable of probing presently unreachable regions of the parameter space of axions with masses $> 10^{-3}$ (The axion parameter space is the yellow highlighted region inFig. 2). IAXO will employ a superconducting toroidal magnet with eight bores, each with their own detector and optic. BabyIAXO's superconducting magnet will have two bores, and thus two detectors and optics [1]. IAXO will achieve new limits of sensitivity by optimizing the magnet, detector, and optics for this rare signal search. With increased cross-sectional area, length, and field strength, the magnet is able to convert more axions into photons. Due to the expected low signal, the detectors of IAXO must have a low background, necessitating a small area. The optics must be able to focus converted photons from the large magnet onto the small detector, losing as few photons as possible in the process.

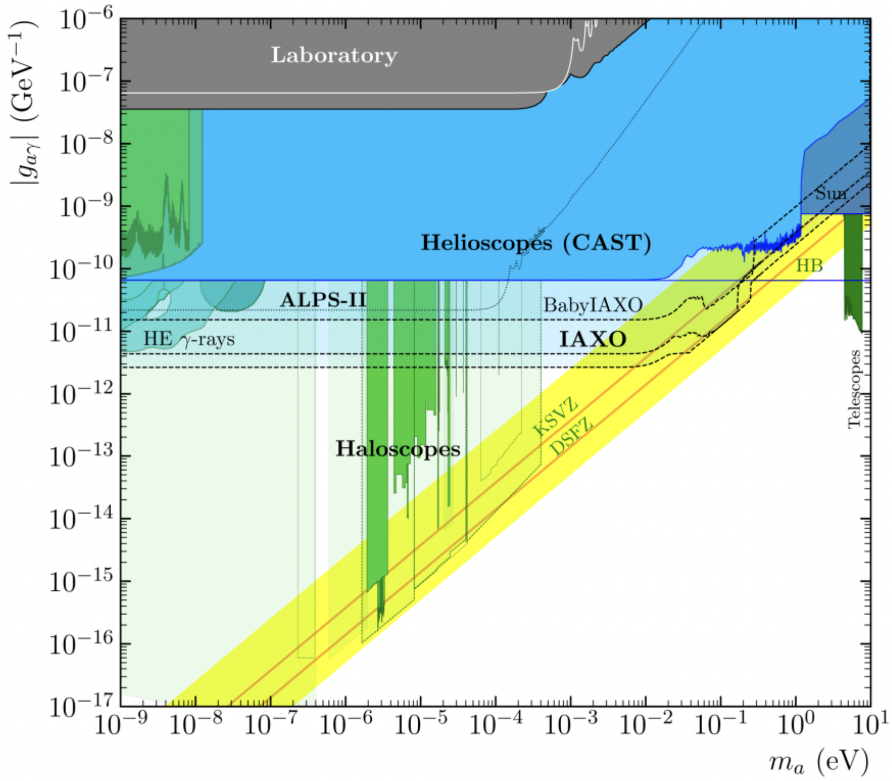

Figure 2: *Parameter Plot of Axion Properties with exclusions confirmed by previous experiments [1]*

The optics of BabyIAXO and IAXO will build upon a strong base of knowledge from previous X-ray telescope experiments. One of the two optics for BabyIAXO will use the flight spare optic from the European Space Agency's XMM-Newton mission. The other optic will be custom-made for BabyIAXO and IAXO, featuring an inner and outer optic constructed of segmented slumped glass. The Perez Lab at Columbia University will contribute the inner optic, and will adapt assembly techniques used by the NuSTAR mission that Columbia also contributed to.

1.3 X-ray Optics

The IAXO and BabyIAXO optics will utilize a Wolter-1 telescope design in order to reflect X-ray photons at grazing incidence angles. X-rays are absorbed at normal incidence angles, and reflect best at extremely shallow angles. Wolter-1 telescopes consist of a curved paraboloid primary mirror angled less than one degree from the direction of incoming light and a curved hyperboloid secondary mirror angled a few more degrees. This design allows X-rays to be slightly

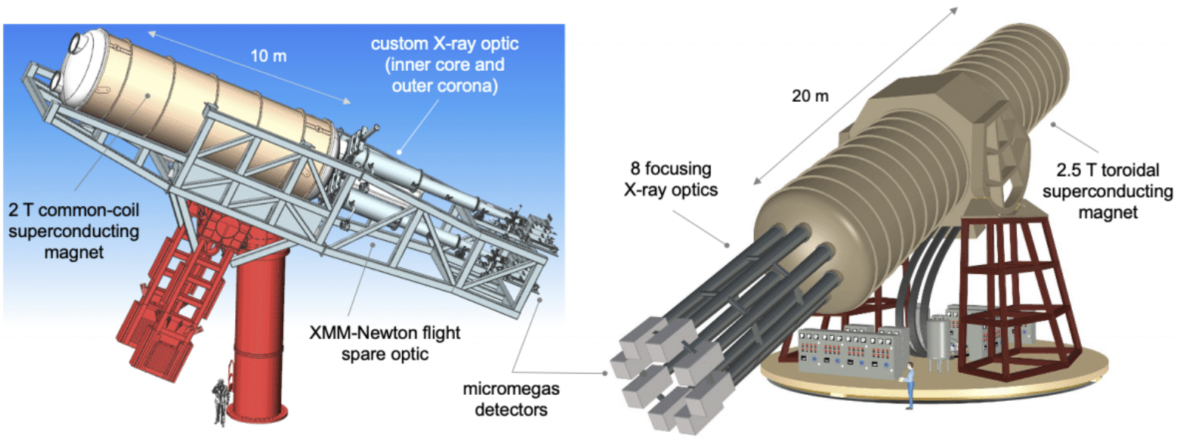

Figure 3: *Models of BabyIAXO (left) and IAXO (right) [1]*

redirected with low loss, focusing to a location several meters away. Due to the required shallow angles, the collection area for a pair of primary and secondary mirrors is limited to very close to the primary mirror's surface. In order to increase collection area, mirrors are stacked in concentric layers increasing in radius [6].

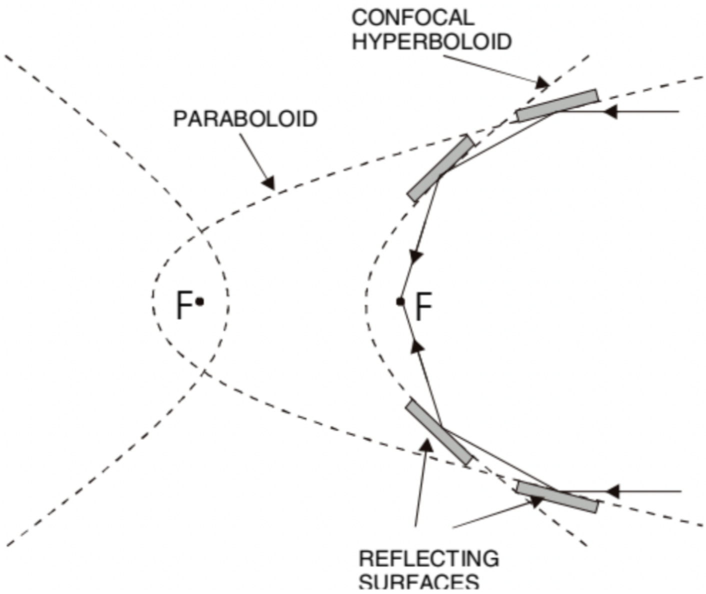

Figure 4: *Wolter-1 telescope schematic [6]*

The custom inner optic for BabyIAXO will consist of 97 inner layers ranging in radius from $50mm$ to $400mm$. The outer optic will have 26 layers, adding collection area at radii $400mm$ to $700mm$. The outer optic will be constructed with novel cold slumping glass technology, which is ideal for glass that has to bend minimally. The inner optic will use heat-slumped glass to achieve its more severe curvature.

1.4 Optic Assembly

Significant infrastructure from the construction of the NuSTAR optic remains at Columbia, and the inner optic for IAXO has been intentionally designed to take advantage of existing materials. The IAXO and NuSTAR optic are the same length and cover the same range of radii, although IAXO will have 36 fewer layers. BabyIAXO and IAXO hope to repurpose many of the over 7000 pieces of glass that were made for NuSTAR but not used on the final optics. The

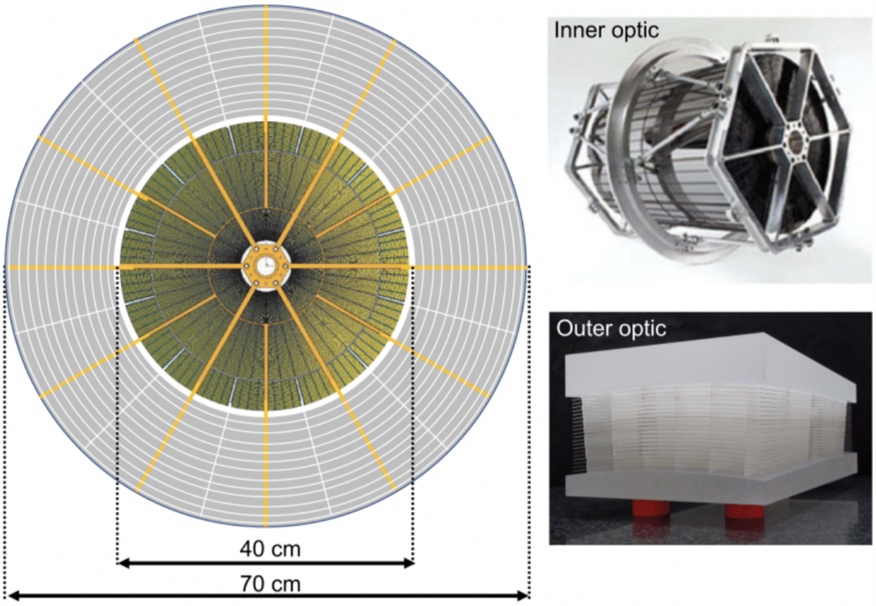

Figure 5: *Left: Schematic of the custom BabyIAXO optic. Right Top: The NuSTAR optic that serves as the basis for the inner optic assembly process. Right Bottom: The cold slumping process that will be used for the outer optic. [1]*

assembly process for the IAXO optic will closely resemble the process employed for NuSTAR. Both missions utilize the technique of thermal forming to achieve the curved glass required for the optic. Each thermally formed cylindrical shaped piece of glass is then scanned by a laser profilometer [2]. The laser profilometer measures the roughness of the reflecting surface of the piece and predicts the half power diameter (HPD) that an optic made with that piece would return. The half power diameter of an optic is the diameter at which half of the light focused by the optic would be enclosed in a circle, a central measure of imaging performance to ensure that as much light as possible reaches IAXO's detector [3]. After laser scanning to verify quality, the piece is cut to the specific dimensions required for the optic. The glass is then sent to the Technical University of Denmark (DTU) where a multilayer reflective coating is applied. This coating is optimized to reflect as many X-ray photons as possible, with each layer designed to reflect photons that are not reflected by higher layers. After coating, pieces return to the laser profilometer to detect any changes in roughness created during the coating process. Next, each layer of the optic is assembled layer by layer via an error-correcting monolithic assembly and alignment (EMAAL) machine, which bends each piece of glass from its cylindrical shape into the conical shape desired for the optic and eliminates figure errors. Finally, each layer undergoes linear variable differential transformer (LVDT) characterization to measure how much light each layer of the optic can reflect [2].

2 Thermal Slumping

2.1 Slumping Theory

The first step of the BabyIAXO optic assembly is curving each glass piece into a cylindrical shape via thermal slumping. During thermal slumping, a piece of glass is placed in an oven on top of a concave cylindrical quartz mandrel. The glass is heated until it slowly slumps down into the mold, assuming its cylindrical shape. Throughout the process, the glass sheet maintains contact with the mandrel only along the sides of the piece (labeled "contact lines" in Fig. 6). This ensures the figure and roughness of the piece are minimally deformed during slumping with the inner surface of the cylinder, the eventual reflective surface of the optic, never coming into contact with the mandrel and avoiding surface deformation [4]. In order to preserve the ideal figure with minimal roughness, each piece should be neither underslumped or overslumped. Underslumping occurs when the piece does not sink far enough into the mandrel and does not take on the appropriate curvature for the layer. Overslumping occurs when the piece is heated for long enough that it has fully settled on the bottom of the mandrel, possibly taking on surface imperfections present in the mandrel. Ideally, the glass should hover just above the bottom of the mandrel as shown in Fig. 6 (4).

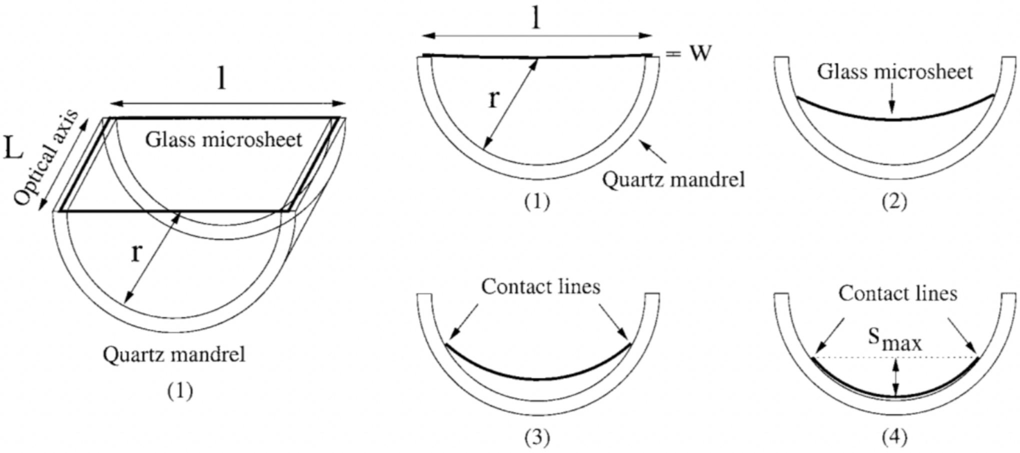

Figure 6: *(1) Diagram slumping setup with glass sheet on top of a cylindrical quartz mandrel. (2-4) Slumping process at various time intervals as the glass sinks down the sides of the mandrel and takes on its cylindrical shape [4].*

Achieving an ideal slump requires careful manipulation of variables within the framework of a slumping recipe. During the heating process, the rate, temperature, and time that a piece is heated at are all variables for the ovens at Nevis Laboratories. A slumping recipe also accounts for important phases in the heating process that correspond with specific viscosities of the glass. The strain point of the glass is where the glass reaches a low enough viscosity where it is no longer elastic and it's shape can be permanently changed. After this point, the glass will begin to slump. In order to prevent uneven slumping across the piece, the oven is held at the temperature corresponding to the strain point for several minutes. This hold thermalizes the oven and decreases any temperature gradients and uneven heating across the oven. Beyond the strain point, the glass is heated to its soak temperature where the majority of the slumping takes place. The soak temperature and the soak time are the strongest determining factors of if the piece will emerge overslumped or underslumped. The softening point of the glass serves as an upper limit for possible soak temperatures, as below the softening point the glass retains its initial thickness across the sheet [4]. The strain temperature, soak temperature, thermalization time, soak time, and rate of heating before and after thermalization are all variable within the slump recipe, as seen in the schematic Fig. 7.

During the construction of the High-Energy Focusing Telescope (HEFT) a viscodynamic model (1) for the strain on a piece of glass was derived in Jimenez-Garate et al.[4]. This model finds the relationship between the viscosity and the soak time necessary to achieve an ideal slump.

$$\frac{\eta_{soak}}{t_{soak}} = \frac{5C\rho g l^4}{64 s_{max}(1+\nu)\omega^2} \quad (1)$$

This relationship relies on the properties of the type of glass as well as the size of the piece and how gravity will pull the sheet into the mandrel during the slumping process. Viscosity

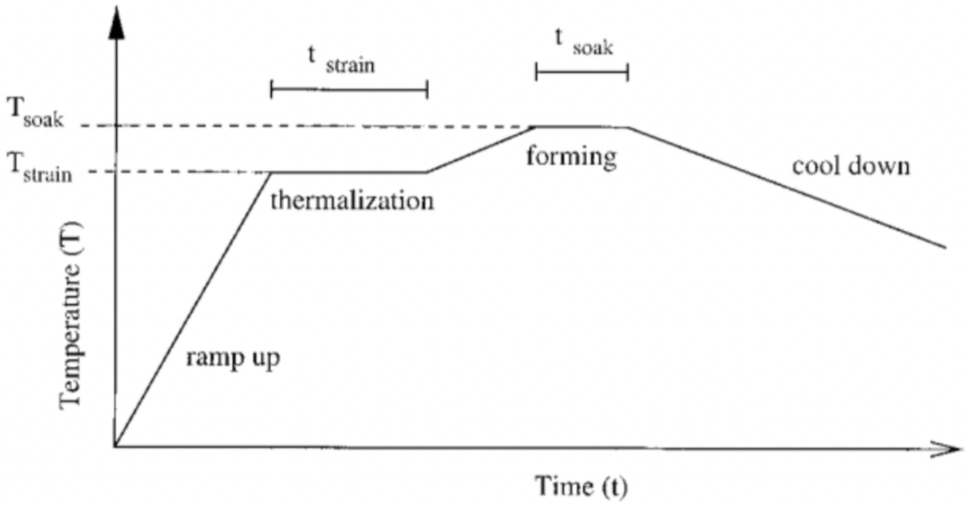

Figure 7: *Slump recipe schematic [4].*

and temperature are inversely related, so the model is able to directly inform slumping recipes, pinpointing soak temperatures and times that will create ideally slumped pieces.

2.2 Slumping Method

The slumping procedure was defined by the specifications of the Schott D263 glass used for the substrates. The D263 glass is $0.2mm$ thick. Each piece was cut to a length between $200mm$ and $225mm$, $225mm$ being the length required for IAXO and used for NuSTAR, with shorter pieces used to maximize the amount of glass that could be used from each original pane of glass [2]. Each piece was cut to a width $3mm$ wider than the radius of the mandrel it would be slumped in.

In order to evaluate the figure of each slumped piece, the piece underwent a three phase inspection. The skew of the piece was measured by placing the piece on a table in a convex orientation and measuring any distance between one corner of the sheet and the table when the three other corners were held to the surface. Pieces were inspected for any visible divots on the inner reflection surface. The diameter at the front of the piece was compared to the diameter at the back of the piece to identify uneven slumping. A differential in diameter indicated that a piece was underslumped with the front of the piece slumping slower due to its proximity to the oven door and not taking on the ideal curvature. A high skew was experimentally associated with overslumping. In order for a piece to be classified as a case of ideal slumping, no divots could be present, and skew and diameter differential had to be measured as $< 0.5mm$.

The slumping procedure was split into three phases. First, all glass was heated to a temperature of $310°C$ at a rate of $15°C$ per minute. Then, the rate of heating was decreased to $9°C$ per minute until the oven reached the strain point of $529°C$ for Schott D263 glass. Two thermalization times were used in experiments. Trials with a ten minute thermalization period produced pieces with lower skews than those with a three minute thermalization period, and the ten minute thermalization period was quickly adopted as standard. The soak temperature and soak time is related to the size of the piece, with larger pieces slumping faster or at lower temperatures as gravity overcomes the force of the mandrel holding the glass up at the contact points.

2.3 Experimental Results

In total, 70 pieces of glass were thermally slumped, across four different mandrels with diameters ranging from $91mm$ to $155mm$. 25 of these pieces passed visual inspection and are considered ideal slumps. Out of 43 trials, only 5 ideally slumped pieces were formed without incorporating the viscodynamic model from Jimenez-Garate et al. [4] into slump recipe predictions, a success rate of 11.6%. 20 of the 27 pieces slumped with recipes informed by the model passed visual inspection, a success rate of 74.1%. The use of the model to inform slump recipes has been incredibly successful for multiple mandrel diameters. Fig. 8, 9, and 10 compare the viscosity and time relationship for an ideal slump with results of the trials. According to the model, pieces slumped with a viscosity-time relationship that falls above the line will be underslumped, while pieces slumped with a relationship below the line will be overslumped.

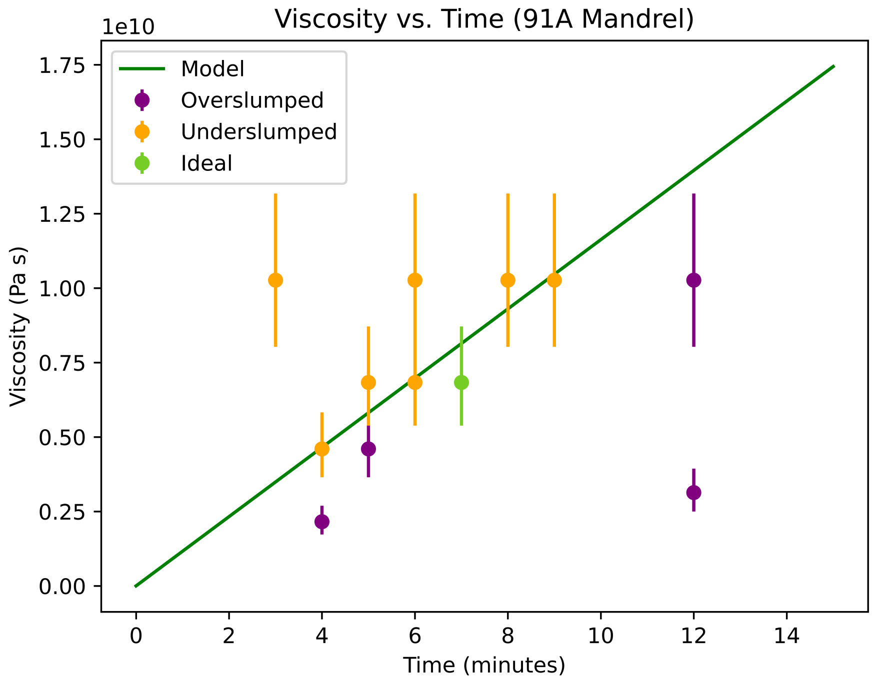

Figure 8: *Viscosity vs. time relationship and experimental trials for 91mm diameter mandrel. The green line is where the model predicts where ideal slumping will take occur. Orange points are underslumped trials, green points are ideally slumped trials, and purple points are overslumped trials.*

The model proved to be largely accurate in its slump recipe predictions, particularly as mandrels increased in size.

3 Future Work and Conclusions

Thermal slumping recipes that repeatably produce high quality cylindrical glass will be essential to the production of optics for BabyIAXO and IAXO. These experimental results demonstrate that Jimenez-Garate's [4] model predicts reliable slump recipes that can be methodically extended to the full range of radii required for the optic. Trials that incorporated model predictions were successful more than six times as often as trials ran without the model. With each optic requiring over 2000 pieces of glass, modeled recipes will save valuable production time that would otherwise be spent identifying successful recipes over the course of multiple trials.

Pieces identified as ideal in these trials should be scanned by the laser profilometer to quantitatively determine the HPD and imaging performance produced by this slumping technique. Characterization of these pieces from the profilometer should directly inform further adaptations to the slumping process. More experimental data across a wider range of mandrel radii would demonstrate how well the model adapts to larger pieces of glass. Experiments that characterize the individual ovens at Nevis Laboratories should be conducted to determine if the ovens, each of

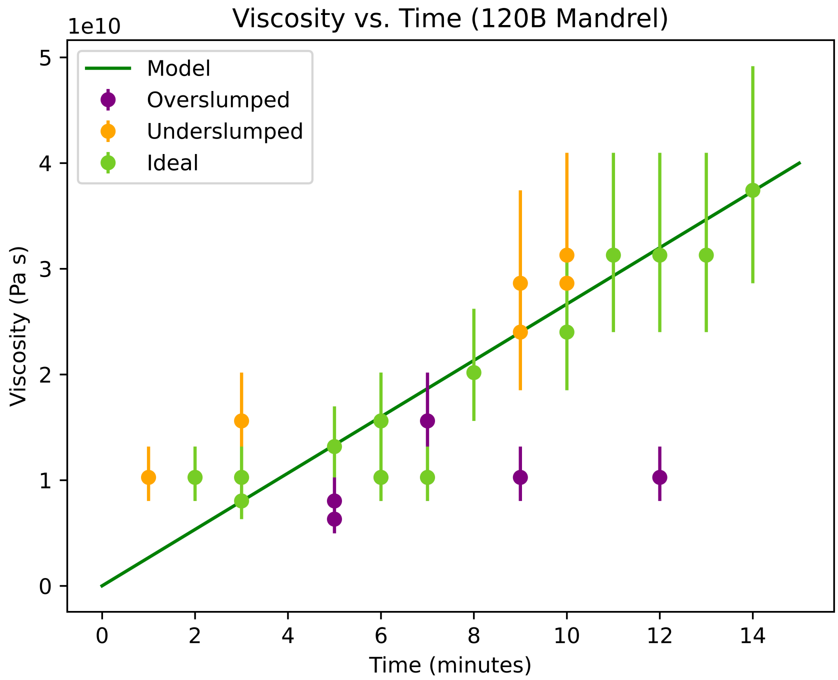

Figure 9: *Viscosity vs. time relationship and experimental trials for* 120*mm diameter mandrel. The green line is where the model predicts where ideal slumping will take occur. Orange points are underslumped trials, green points are ideally slumped trials, and purple points are overslumped trials.*

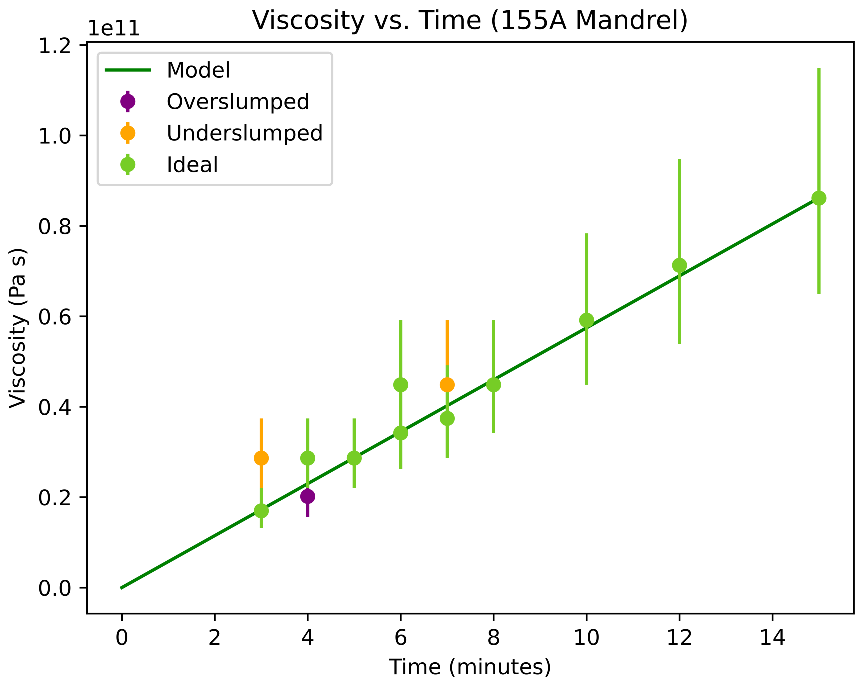

Figure 10: *Viscosity vs. time relationship and experimental trials for* 155*mm diameter mandrel. The green line is where the model predicts where ideal slumping will take occur. Orange points are underslumped trials, green points are ideally slumped trials, and purple points are overslumped trials.*

which is over 15 years old, are reporting accurate temperatures and have limited thermal gradients across their dimensions. Work to devise an thermocouple setup for these measurements has begun, but requires further testing for accurate readings.

BabyIAXO is set to begin operations starting in 2028, with construction of its core optic to begin in 2025 [1]. Informed by the experimental results of this work, the first step of optic production can begin with confidence, utilizing reliable recipes to create the cylindrically shaped glass required for the optic design, with a success rate near 75%.

4 Acknowledgements

I would like to thank Dr. Kerstin Perez, Mike Law, and Marcela Stern for their guidance and support throughout this project. I would also like to thank Dr. Georgia Karagiorgi, Dr. Reshmi Mukherjee, and Amy Garwood for their support of this REU Program. This material is based upon work supported by the National Science Foundation under Grant No. PHY-2349438.

References

[1] The IAXO Collaboration. Conceptual design of babyiaxo, the intermediate stage towards the international axion observatory. *Journal of High Energy Physics*, 2021(5):137, May 2021.

[2] William W. Craig et al. Fabrication of the nustar flight optics. page 81470H, San Diego, California, USA, September 2011.

[3] Mario Jimenez-Garate. The development of hard x-ray telescope optics and a theoretical model of x-ray emission from accretion disks /. January 2001.

[4] Mario A. Jimenez-Garate, Charles J. Hailey, William W. Craig, and Finn E. Christensen. Thermal forming of glass microsheets for x-ray telescope mirror segments. *Applied Optics*, 42(4):724, February 2003.

[5] Chanda Prescod-Weinstein. Enter the axion. *American Scientist*, April 2021.

[6] Paul B. Reid. *Encyclopedia of astronomy and astrophysics*. Institute of Physics Pub.; Nature Pub. Group, Bristol; Philadelphia: London; New York, 2001.